

## CHEMICAL REACTION, ELECTRIFICATION, BROWNIAN MOTION AND THERMOPHORESIS EFFECTS OF COPPER NANOPARTICLES ON NANOFLUID FLOW WITH SKIN FRICTION, HEAT AND MASS TRANSFER

Aditya Kumar Pati<sup>a\*</sup>, Madan Mohan Rout<sup>a</sup>, Runu Sahu<sup>b</sup>, I. Siva Ramakoti<sup>a</sup>,  
Koustava Kumar Panda<sup>a</sup>, Krushna Chandra Sethi<sup>a</sup>

<sup>a</sup>Centurion University of Technology and Management, Paralakhemundi, Odisha, India

<sup>b</sup>NIST University, Berhampur, Ganjam, Odisha, India

\*Corresponding Author e-mail: [apati@cutm.ac.in](mailto:apati@cutm.ac.in)

Received July 2, 2024; revised September 18, 2024; accepted September 23, 2024

This study investigates the effects of first-order chemical reaction, thermophoresis, electrification, and Brownian motion on *Cu* nanoparticles within a free convective nanofluid flow past a vertical plane surface, focusing on skin friction, heat and mass transfer. The unique combination of chemical reaction and electrification effects sets this study apart from previous research on nanofluid flow. By utilizing similarity functions, the governing PDEs of the flow are converted into a system of locally similar equations. These equations are then solved using MATLAB's `bvp4c` function, incorporating dimensionless boundary conditions. The findings are verified through a comparison with previous studies. Graphical illustrations show the numerical explorations for concentration, velocity, and temperature profiles in relation to the electrification parameter, thermophoresis parameter, chemical reaction parameter, and Brownian motion parameter. The computational results for heat transfer, mass transfer and dimensionless skin friction coefficients are presented in tabular form. The primary finding indicates that the electrification parameter accelerates heat transfer, while the electrification parameter, Brownian motion parameter, and chemical reaction parameter enhance the rate of mass transfer from the plane surface to the nanofluid. This indicates encouraging potential for cooling plane surfaces in manufacturing industries.

**Keywords:** *Chemical Reaction; Thermophoresis; Electrification; Brownian Motion; Nanofluid*

**PACS:** 47.70.Fw, 44.20.+b, 44.25.+f, 47.10.ad, 47.15.Cb

### Nomenclature

<p><math>c</math> specific heat capacity</p> <p><math>C</math> local concentration</p> <p><math>C_f</math> Local skin friction coefficient</p> <p><math>D_B</math> Brownian diffusion coefficient</p> <p><math>D_T</math> Thermophoresis diffusion coefficient</p> <p><math>(E_x, E_y)</math> electric intensity components</p> <p><math>f</math> dimensionless stream function</p> <p><math>F</math> time constant for momentum transfer between the fluid and nanoparticles</p> <p><math>g</math> gravitational acceleration</p> <p><math>k</math> thermal conductivity</p> <p><math>k_1</math> rate of chemical reaction</p> <p><math>m</math> nanoparticle mass</p> <p><math>M</math> electrification parameter</p> <p><math>Nb</math> Brownian motion parameter</p> <p><math>Nc</math> concentration ratio</p> <p><math>N_F</math> momentum transfer number</p> <p><math>Nr</math> buoyancy ratio</p> <p><math>N_{Re}</math> electric Reynolds number</p> <p><math>Nt</math> thermophoresis parameter</p> <p><math>Nu_x</math> local Nusselt number</p> <p><math>Pr</math> Prandtl number</p> <p><math>q</math> charge of the nanoparticle</p>	<p><math>Ra_x</math> local Rayleigh number</p> <p><math>s</math> dimensionless concentration</p> <p><math>Sc</math> Schmidt number</p> <p><math>Sh_x</math> local Sherwood number</p> <p><math>T</math> local temperature</p> <p><math>(u, v)</math> velocity components</p> <p><math>\alpha</math> thermal diffusivity</p> <p><math>\beta_f</math> volumetric thermal expansion coefficient</p> <p><math>\epsilon_0</math> permittivity</p> <p><math>\eta</math> similarity variable</p> <p><math>\gamma</math> chemical reaction parameter</p> <p><math>\mu</math> dynamic viscosity</p> <p><math>\theta</math> temperature in dimensionless form</p> <p><math>\rho</math> density</p> <p><math>\nu</math> kinematic viscosity</p> <p><math>\psi</math> stream function</p> <p><b>Subscripts</b></p> <p><math>s</math> nanoparticle phase</p> <p><math>nf</math> nanofluid phase</p> <p><math>f</math> base fluid phase</p> <p><math>w</math> condition at the plane surface</p> <p><math>\infty</math> free stream condition</p>
---	---

### 1. INTRODUCTION

Recent progress in nanoscience arises from exploring the physical properties of matter on the nanoscale. One notable area of industrial application is nanofluids, which have become prominent in the field of heat transfer. These nanofluids have garnered significant attention because of their exceptional thermal transport properties and their fascinating uses across several industries. The motivation for researching nanofluids stems from the improved heat transfer in applications such as nuclear engineering, computer processor microchips, air conditioning and refrigeration systems, space cooling, micromanufacturing, and fuel cells. The classical theory of single-phase fluids can be adapted for nanofluids by treating

their thermophysical properties as dependent on both the base fluids and their individual components. It is crucial to recognize that factors such as thermal conductivity, volume fraction, particle size, and temperature all play a role in enhancing the thermal conductivity of nanofluids. Buongiorno [1] formulated a dual-phase framework aimed at investigating thermal energy transfer utilizing nanofluids. Subsequently, Tiwari and Das [2] introduced a more streamlined approach where the thermophysical characteristics varied with the nanoparticle volume fraction. These models have proven highly effective in addressing diverse flow challenges related to nanofluids. For example, Kuznetsov and Nield [3] were the first to use the Buongiorno model to study the effects of thermophoresis and Brownian motion on free convective nanofluid flow near a vertical plate. Since then, numerous researchers (Khan and Aziz [4], Ibrahim and Makinde [5], Khan et al. [6], Ganga et al. [7], Mohamed et al. [8], Goyal and Bhargava [9], Rana et al. [10], and Dey et al. [11]) have examined the impacts of Brownian motion and thermophoresis on nanofluid flow past a plate surface. Some researchers (Dey et al. [11], Padmaja and Kumar [12], Padmaja and Kumar [13], Dey et al. [14]) have recently reported on the influences of chemical reaction on nanofluids.

The effect of electrification on nanofluid flow has recently garnered significant interest. The pioneering examination of the improvement in heat and mass transfer due to nanoparticle electrification was conducted by Pati et al. [15] in a study of nanofluid flow over a stretching cylinder. Further investigations into the impact of nanoparticle electrification on nanofluid flow have been carried out by researchers such as Panda et al. [16], Pati et al. [17, 18] and Pattanaik et al. [19]. In a more recent study, Pati et al. [20] explored the effects of electrified nanoparticles and the electric Reynolds number on nanofluid flow past a vertical flat surface, concluding that the electrification mechanism significantly enhances both heat and mass transfer.

Previous studies have rarely explored the impact of nanoparticle electrification on nanofluid flow. Additionally, there are no existing studies that consider both electrification and chemical reaction effects on nanofluid flow. This study aims to investigate the combined effects of electrification and chemical reaction on the free convective flow of  $Cu$ -water nanofluid past a vertical plane surface. It incorporates Brownian motion and thermophoresis, using Buongiorno’s model.

## 2. MATHEMATICAL FORMULATION

A laminar incompressible steady free convective flow is analyzed, with the vertical plane surface aligned along the  $x$ -axis. The plane surface consistently maintains fixed values for both concentration ( $C_w$ ) and temperature ( $T_w$ ). A schematic representation is shown in Fig. 1.

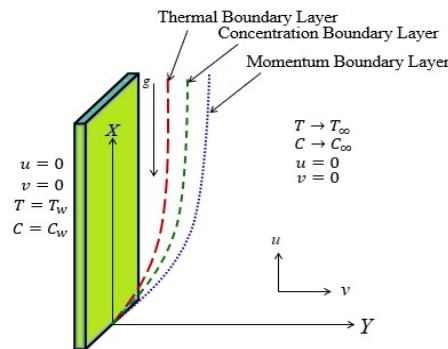


Figure 1. Schematic representation

The governing equations (Pati et al. [21]) incorporating first-order chemical reaction, thermophoresis, electrification, and Brownian motion, and utilizing the Oberbeck-Boussinesq approach, can be formulated as follows:

$$\frac{\partial u}{\partial x} + \frac{\partial v}{\partial y} = 0, \tag{1}$$

$$u \frac{\partial u}{\partial x} + v \frac{\partial u}{\partial y} = \frac{\mu_{nf}}{\rho_{nf}} \left( \frac{\partial^2 u}{\partial y^2} \right) + \frac{\rho_s}{\rho_{nf}} \frac{q}{m} E_x (C - C_\infty) + \frac{\rho_{f\infty}}{\rho_{nf}} (1 - C_\infty) \beta_{f\infty} g (T - T_\infty) - \frac{1}{\rho_{nf}} (C - C_\infty) (\rho_s - \rho_{f\infty}) g, \tag{2}$$

$$u \frac{\partial T}{\partial x} + v \frac{\partial T}{\partial y} = \frac{(\rho c)_s}{(\rho c)_{nf}} D_B \frac{\partial C}{\partial y} \frac{\partial T}{\partial y} + \frac{(\rho c)_s}{(\rho c)_{nf}} \frac{q}{m} F \left( E_x \frac{\partial T}{\partial x} + E_y \frac{\partial T}{\partial y} \right) + \frac{k_{nf}}{(\rho c)_{nf}} \left( \frac{\partial^2 T}{\partial y^2} \right) + \frac{(\rho c)_s}{(\rho c)_{nf}} \frac{D_T}{T_\infty} \left( \frac{\partial T}{\partial y} \right)^2, \tag{3}$$

$$u \frac{\partial C}{\partial x} + v \frac{\partial C}{\partial y} = \frac{D_T}{T_\infty} \frac{\partial^2 T}{\partial y^2} + D_B \frac{\partial^2 C}{\partial y^2} + \left( \frac{q}{m} \right) \frac{1}{F} \left[ \frac{\partial(C E_x)}{\partial x} + \frac{\partial(C E_y)}{\partial y} \right] - k_1 (C - C_\infty), \tag{4}$$

along with the boundary conditions:

$$\left. \begin{aligned} y = 0, \quad v = 0, u = 0, \quad T = T_w, \quad C = C_w \\ y \rightarrow \infty, \quad v = 0, u = 0, \quad T \rightarrow T_\infty, C \rightarrow C_\infty \end{aligned} \right\} \tag{5}$$

The electric field equation is expressed as follows:

$$\frac{\partial E_y}{\partial y} = \frac{\rho_s}{\epsilon_0} \frac{q}{m}. \tag{6}$$

The equations are converted into a non-dimensional format by defining the following dimensionless functions:

$$\psi = (Ra_x)^{\frac{1}{2}} \alpha_f f(\eta), \eta = \frac{y}{x} (Ra_x)^{\frac{1}{4}}, \theta(\eta) = \frac{T-T_\infty}{T_w-T_\infty}, s(\eta) = \frac{C-C_\infty}{C_w-C_\infty}, \quad (7)$$

where  $Ra_x = \frac{(1-C_\infty)x^3(T_w-T_\infty)\beta_f g}{\nu_f \alpha_f}$ .

The stream function, denoted by  $\psi$ , can be defined as follows:

$$v = -\frac{\partial \psi}{\partial x} \text{ and } \frac{\partial \psi}{\partial y} = u. \quad (8)$$

By substituting equations (6), (7), and (8) into equations (1) to (4), the non-dimensional equations are obtained as follows:

$$f''' = -\frac{\phi_1}{4Pr} [3ff'' - 2(f')^2] - \frac{\phi_1 \phi_2 M Nb Sc}{Pr N_F} s - \frac{1}{\phi_5} (\theta - Nr s), \quad (9)$$

$$\theta'' = -\frac{1}{\phi_4} Pr Nt (\theta')^2 - \frac{1}{\phi_4} Sc Nb \left[ \frac{N_F}{N_{Re}} - \frac{1}{4} M \right] (s + Nc) \eta \theta' - \frac{1}{\phi_4} Pr Nbs' \theta' - \frac{3}{4} \frac{1}{\phi_3 \phi_4} f \theta', \quad (10)$$

$$s'' = -\frac{Nt}{Nb} \theta'' + \frac{1}{4} \frac{M Sc}{Pr} \eta s' - \frac{N_F Sc}{Pr N_{Re}} (\eta s' + s + Nc) + \frac{Sc}{Pr} \gamma s - \frac{3}{4} \frac{Sc}{Pr} f s', \quad (11)$$

where prime (') denotes differentiation with respect to  $\eta$ .

The equations (5) are transformed to

$$\left. \begin{aligned} At \eta = 0, f = 0, f' = 0, \theta = 1, s = 1 \\ As \eta \rightarrow \infty, f' \rightarrow 0, \theta \rightarrow 0, s \rightarrow 0 \end{aligned} \right\} \quad (12)$$

The nondimensional parameters are represented as

$$\begin{aligned} \gamma &= \frac{k_1 x}{\alpha_f (Ra_x)^{\frac{1}{2}}}, M = \left(\frac{q}{m}\right) \frac{1}{F \left(\frac{\alpha_f (Ra_x)^{\frac{1}{2}}}{x}\right)} E_x, Nb = \frac{(\rho c)_s D_B (C_w - C_\infty)}{(\rho c)_f \nu_f}, Nt = \frac{(\rho c)_s D_T (T_w - T_\infty)}{(\rho c)_f \nu_f T_\infty}, N_F = \frac{\left(\frac{\alpha_f (Ra_x)^{\frac{1}{2}}}{x}\right)}{F x}, \\ Nr &= \frac{(\rho_s - \rho_f)(C_w - C_\infty)}{(1 - C_\infty) \rho_f \beta_f (T_w - T_\infty)}, Sc = \frac{\nu_f}{D_B}, Nc = \frac{C_\infty}{(C_w - C_\infty)}, Pr = \frac{\nu_f}{\alpha_f}, \frac{1}{N_{Re}} = \left(\frac{q}{m}\right)^2 \frac{\rho_s}{\epsilon_0} \frac{x^2}{\left(\frac{\alpha_f (Ra_x)^{\frac{1}{2}}}{x}\right)^2}. \end{aligned}$$

The thermophysical constants  $\phi_1, \phi_2, \phi_3, \phi_4$  and  $\phi_5$  are expressed according to Pati et al. [20]. This study employs a nanofluid with a 1% concentration of *Cu* nanoparticles. The thermophysical properties of both pure water and the nanoparticles are assessed following the data provided by Oztop and Abu-Nada [22].

$C_f, Nu_x$  and  $Sh_x$  are presented for use in skin friction, heat and mass transfer applications as follows:

$$\begin{aligned} C_f &= \frac{x^2 \tau_w}{\mu_f \alpha_f (Ra_x)^{\frac{3}{4}}}, \text{ where } \tau_w = \mu_f \left(\frac{\partial u}{\partial y}\right)_{y=0}, \\ Nu_x &= \frac{x q_w}{(T_w - T_\infty) k_f}, \text{ where } q_w = -k_f \left(\frac{\partial T}{\partial y}\right)_{y=0}, \\ Sh_x &= \frac{x q_m}{(C_w - C_\infty) D_B}, \text{ where } q_m = -D_B \left(\frac{\partial C}{\partial y}\right)_{y=0}. \end{aligned}$$

The reduced skin friction coefficient ( $f''(0)$ ), heat transfer coefficient ( $-\theta'(0)$ ) and mass transfer coefficient ( $-s'(0)$ ) in non-dimensional form are expressed as follows:

$$C_f = f''(0), -\theta'(0) = Nu_x / Ra_x^{1/4}, -s'(0) = Sh_x / Ra_x^{1/4}.$$

### 3. NUMERICAL SOLUTION AND COMPARISON OF RESULTS

The MATLAB `bvp4c` function is used to derive numerical solutions of the equations (9) to (11) along with boundary condition (12), which are recognized as local similarity equations since the parameters  $\gamma, M, N_{Re}$  and  $N_F$  depend on  $x$ . Numerical results are considered valid as long as they produce a locally similar solution, as highlighted by Farooq et al. [23]. In this context,  $\gamma, M, N_{Re}$  and  $N_F$  are treated as constants, as per [23].

The computed numerical values of the non-dimensional heat transfer coefficient for a regular fluid without considering chemical reaction, thermophoresis, electrification, or Brownian motion have been compared and validated against the results obtained by Bejan [24]. Table 1 demonstrates a significant agreement between both results.

**Table 1.** Comparison of  $-\theta'(0)$ .

$Pr$	$-\theta'(0)$ [Bejan]	$-\theta'(0)$ [present]
1.0	0.40100	0.40099
10.0	0.46500	0.46267

### 4. ANALYSIS OF RESULTS

The influence of key governing parameters, including  $\gamma$ ,  $Nb$ ,  $M$  and  $Nt$  on the dimensionless profiles of velocity ( $f'(\eta)$ ), temperature ( $\theta(\eta)$ ), and nanoparticle concentration ( $s(\eta)$ ) with respect to  $\eta$  were examined numerically. The findings are illustrated through graphs. Additionally, the impact of these parameters on  $f''(0)$ ,  $-\theta'(0)$  and  $-s'(0)$  is displayed in a table.

#### 4.1 Velocity Profiles

$f'(\eta)$  profiles are shown in Figures 2 to 5. These figures explore the effect of  $\gamma$ ,  $Nb$ ,  $M$  and  $Nt$  on  $f'(\eta)$  against  $\eta$ . Figure 2 shows that dimensionless velocity decreases as  $\gamma$  increases. Figure 3 illustrates that dimensionless velocity increases with  $Nb$  due to the rise in the number of fluid particles colliding with nanoparticles. In Figure 4,  $f'(\eta)$  increases with an increase in  $M$ . Finally, Figure 5 shows that  $f'(\eta)$  increases with an increase in  $Nt$ . This is because the increased thermophoresis force causes nanoparticles to move faster, thereby raising the dimensionless velocity profiles.

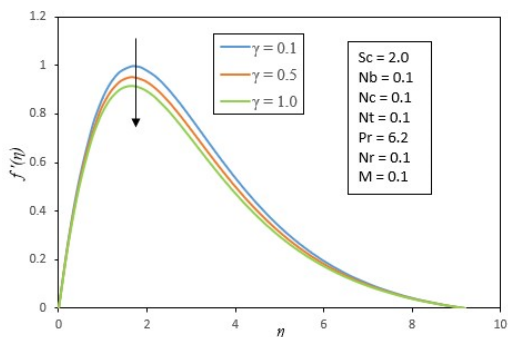


**Figure 2.** Effects of  $\gamma$  on  $f'(\eta)$  when  $N_{Re} = 2.0, N_F = 0.1$

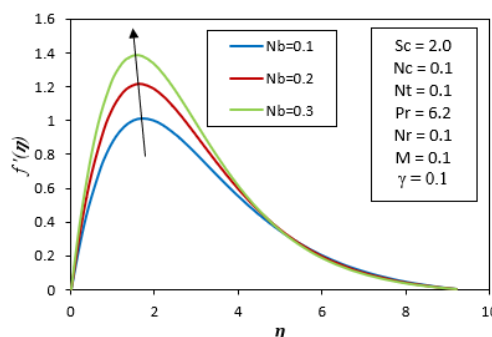


**Figure 3.** Effects of  $Nb$  on  $f'(\eta)$  when  $N_{Re} = 2.0, N_F = 0.1$

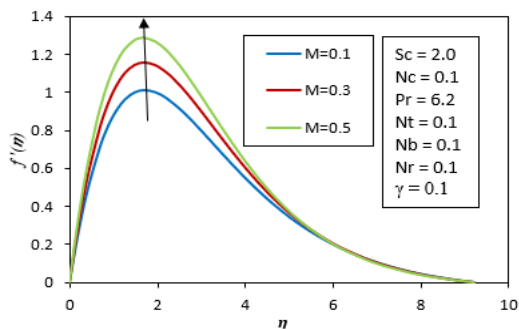


**Figure 4.** Effects of  $M$  on  $f'(\eta)$  when  $N_{Re} = 2.0, N_F = 0.1$

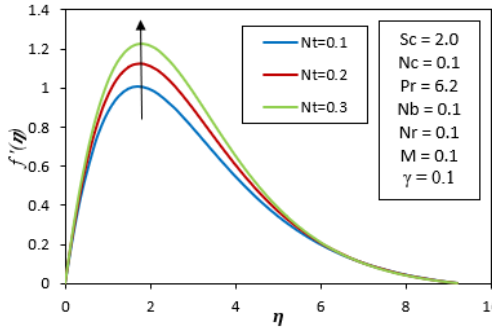


**Figure 5.** Effects of  $Nt$  on  $f'(\eta)$  when  $N_{Re} = 2.0, N_F = 0.1$

#### 4.2 Temperature Profiles

Figures 6 to 9 illustrate  $\theta(\eta)$  profiles corresponding to  $f'(\eta)$  profiles depicted in Figures 2 to 5. In every illustration, the surface's peak temperature is standardized to one, gradually diminishing to the free stream temperature ( $\theta = 0$ ) at the thermal boundary layer's outer edge.

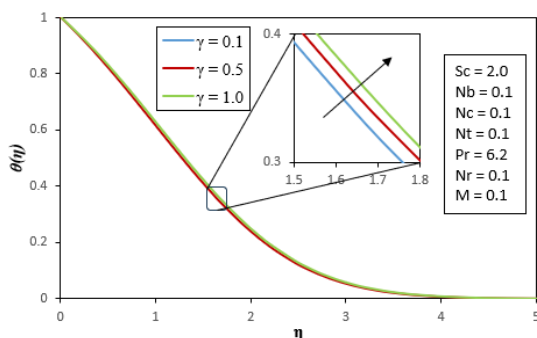


**Figure 6.** Effects of  $\gamma$  on  $\theta(\eta)$  when  $N_{Re} = 2.0, N_F = 0.1$

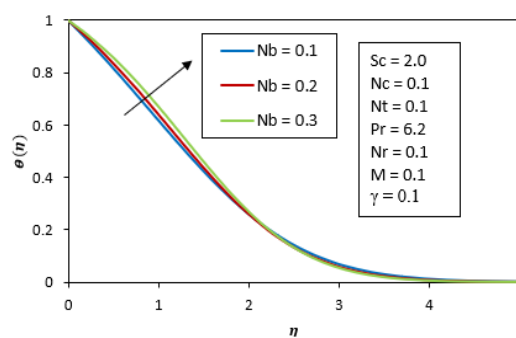


**Figure 7.** Effects of  $Nb$  on  $\theta(\eta)$  when  $N_{Re} = 2.0, N_F = 0.1$

Figure 6 shows the temperature profiles for  $\gamma$ , while Figure 7 demonstrates the impact of  $Nb$ . Increasing  $\gamma$  slightly enhances the dimensionless temperature, as depicted in Fig. 6. Figure 7 illustrates that increasing  $Nb$  enhances temperature, attributed to increased diffusion of nanoparticles due to higher Brownian motion. The presence of nanoparticles induces Brownian motion in the nanofluid, which intensifies with higher  $Nb$  values. This motion enhances thermal conduction through two mechanisms: direct heat transfer via nanoparticles and indirect micro-convection around them. Brownian motion exerts significant influence on small particles under high  $Nb$  conditions, whereas it has the opposite effect on large particles under low  $Nb$  conditions. Figure 8 reveals that increasing  $M$  decreases  $\theta(\eta)$ . The parameter  $Nt$ , highlighted in Figure 9, enhances thermophoresis force, prompting nanoparticles to migrate from warmer to cooler regions and amplifying temperature profiles.

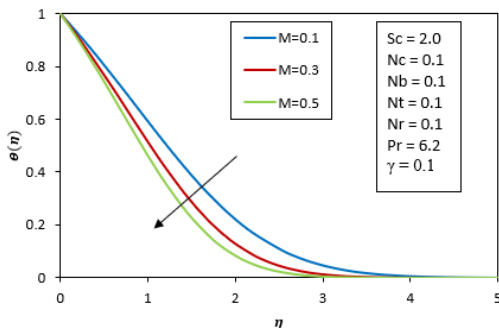


Figure 8. Effects of  $M$  on  $\theta(\eta)$  when  $N_{Re} = 2.0, N_F = 0.1$

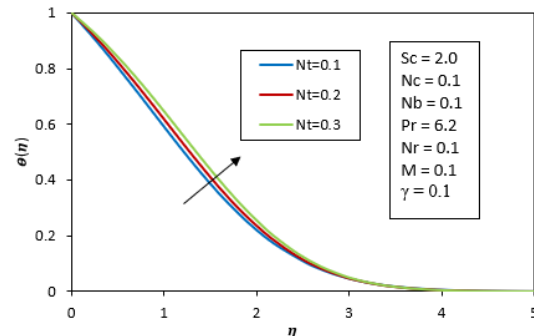


Figure 9. Effects of  $Nt$  on  $\theta(\eta)$  when  $N_{Re} = 2.0, N_F = 0.1$

### 4.3 Concentration Profiles

Figures 10 to 13 illustrate the impact of  $\gamma$ ,  $Nb$ ,  $M$  and  $Nt$  on  $s(\eta)$ . Figure 10 shows that  $s(\eta)$  decreases with increasing  $\gamma$ . Figure 11 demonstrates that as  $Nb$  increases, the concentration of nanoparticles decreases, primarily due to enhanced Brownian motion warming the boundary layer and leading to increased nanoparticle deposition away from the fluid region (onto the plane surface), thus reducing  $s(\eta)$ . Figure 12 indicates that nanoparticle concentration decreases with increasing  $M$ , attributed to heightened electrification causing nanoparticles to migrate from the fluid region towards the plane surface, thereby lowering their concentration. Figure 13 reveals that increasing  $Nt$  results in higher nanoparticle concentration, as greater  $Nt$  intensifies forces on nanoparticles away from the heated plane surface, enhances nanoparticle diffusion into the nanofluid region, and ultimately increases concentration magnitude.

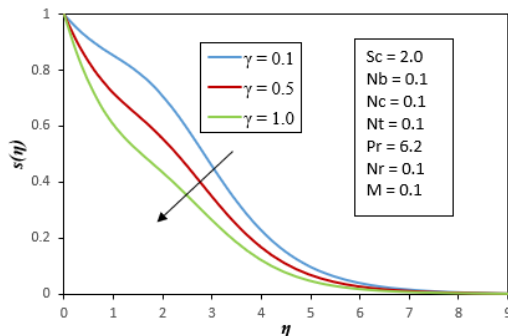


Figure 10. Effects of  $\gamma$  on  $s(\eta)$  when  $N_{Re} = 2.0, N_F = 0.1$

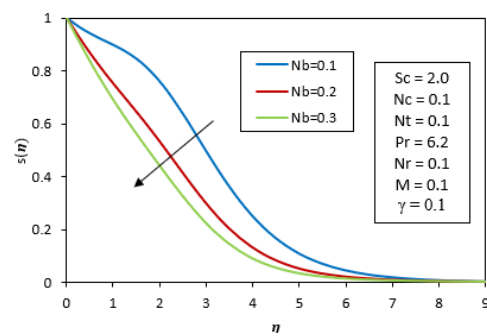


Figure 11. Effects of  $Nb$  on  $s(\eta)$  when  $N_{Re} = 2.0, N_F = 0.1$

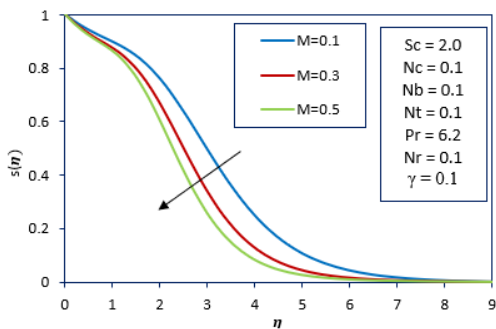


Figure 12. Effects of  $M$  on  $s(\eta)$  when  $N_{Re} = 2.0, N_F = 0.1$

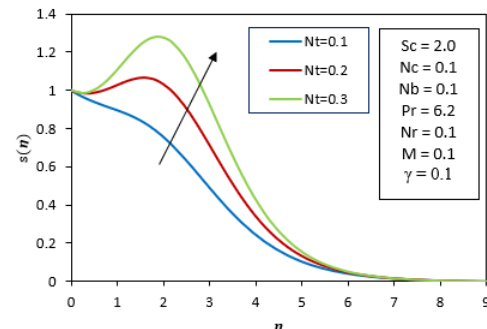


Figure 13. Effects of  $Nt$  on  $s(\eta)$  when  $N_{Re} = 2.0, N_F = 0.1$

### 4.4 Non-dimensional Skin Friction, Heat and Mass Transfer Coefficients

Table 2 illustrates how changes in  $\gamma$ ,  $M$ ,  $Nb$  and  $Nt$  affect  $f''(0)$ ,  $-\theta'(0)$  and  $-s'(0)$  while keeping other parameters fixed ( $Sc = N_{Re} = 2.0, N_F = Nr = Nc = 0.1$  and  $Pr = 6.2$ ).  $f''(0)$  increases with higher values of  $M, Nb$

and  $Nt$ , but decreases as  $\gamma$  rises. This trend is attributed to the velocity distribution near the plane surface, which intensifies with  $M, Nb$  and  $Nt$ , but diminishes with  $\gamma$ . Similarly,  $-\theta'(0)$  increases as  $M$  rises and decreases with higher values of  $\gamma, Nb$  and  $Nt$ . This trend occurs because increasing  $M$  reduces the temperature distribution near the surface, whereas higher values of  $\gamma, Nb$  and  $Nt$  enhance temperature. Values of  $-s'(0)$  increases with  $\gamma, M$ , and  $Nb$ , but decreases with increasing  $Nt$ . This pattern arises because the nanoparticle concentration near the surface decreases with higher values of  $\gamma, Nb$ , and  $M$ , thereby enhancing  $-s'(0)$ . Conversely, increasing  $Nt$  leads to higher nanoparticle concentrations near the surface, resulting in a decrease in  $-s'(0)$ .

**Table 2.** The effects of  $\gamma, M, Nb$  and  $Nt$  on  $f''(0), -\theta'(0)$  and  $-s'(0)$

$\gamma$	$M$	$Nb$	$Nt$	$f''(0)$	$-\theta'(0)$	$-s'(0)$
0.0	0.1	0.1	0.1	1.41442	0.36235	0.14057
0.1				1.40370	0.35248	0.20466
0.5				1.37049	0.32358	0.41039
1.0				1.34253	0.30120	0.59803
0.1	0.0	0.1	0.1	0.97884	0.30109	0.17498
	0.1			1.40370	0.35248	0.20466
	0.2			1.79457	0.38830	0.22064
	0.3			2.16287	0.41670	0.23155
0.1	0.1	0.1	0.1	1.40370	0.35248	0.20466
		0.2		1.58380	0.32715	0.28574
		0.3		1.75312	0.29981	0.33132
0.1	0.1	0.1	0.1	1.40370	0.35248	0.20466
			0.2	1.45044	0.32904	0.17859
			0.3	1.49351	0.30635	0.17309

## 5. CONCLUSIONS

The influences of some key governing parameters, such as  $\gamma, Nb, M$  and  $Nt$  on velocity, concentration and temperature profiles are graphically demonstrated in free convective nanofluid flow past a plane surface. Numerical results for  $f''(0), -\theta'(0)$  and  $-s'(0)$  are highlighted in tabular form. The study yields the following conclusions:

- An increase in  $Nb, Nt$  and  $M$  enhances velocity within the boundary layer, while velocity reduces with increasing  $\gamma$ .
- Higher values of  $Nb, Nt$  and  $\gamma$  intensify temperature, whereas increasing  $M$  reduces temperature.
- Increasing  $Nt$  enhances concentration, whereas  $Nb, \gamma$  and  $M$  lead to decreased concentration.
- $Nb, Nt$  and  $M$  all enhance the dimensionless reduced skin friction coefficient, while  $\gamma$  reduces it.
- The dimensionless heat transfer coefficient diminishes with increasing  $Nb, Nt$  and  $\gamma$ , but significantly rises with an increase in  $M$ .
- The rate of heat transfer from the plane surface to nanofluid rises with increasing  $M$  and conducts heat into the cooler fluid, cooling the plane surface.
- The dimensionless mass transfer coefficient improves with  $\gamma, Nb$  and  $M$  but diminishes with  $Nt$ .

## ORCID

Aditya Kumar Pati, <https://orcid.org/0000-0003-0966-5773>

## REFERENCES

- [1] J. Buongiorno, "Convective transport in nanofluids," ASME J. Heat Transf. **128**, 240-250 (2006). <https://doi.org/10.1115/1.2150834>
- [2] R.K. Tiwari, and M.K. Das, "Heat transfer augmentation in a two-sided lid-driven differentially heated square cavity utilizing nanofluids," Int. J. Heat Mass Transf. **50**, 2002-2018 (2007). <https://doi.org/10.1016/j.ijheatmasstransfer.2006.09.034>
- [3] A.V. Kuznetsov, and D.A. Nield, "Natural convective boundary-layer flow of a nanofluid past a vertical plate," Int. J. Thermal Sci. **49**, 243-247 (2010). <https://doi.org/10.1016/j.ijthermalsci.2009.07.015>
- [4] W.A. Khan, and A. Aziz, "Natural convection flow of a nanofluid over a vertical plate with uniform surface heat flux," Int. J. Therm. Sci. **50**, 1207-1214 (2011). <https://doi.org/10.1016/j.ijthermalsci.2011.02.015>
- [5] W. Ibrahim, and O.D. Makinde, "The effect of double stratification on boundary-layer flow and heat transfer of nanofluid over a vertical plate," Computers & Fluids, **86**, 433-441 (2013). <https://doi.org/10.1016/j.compfluid.2013.07.029>
- [6] W.A. Khan, O.D. Makinde, and Z.H. Khan, "MHD boundary layer flow of a nanofluid containing gyrotactic microorganisms past a vertical plate with Navier slip," International Journal of Heat and Mass Transfer, **74**, 285-291 (2014). <https://doi.org/10.1016/j.ijheatmasstransfer.2014.03.026>
- [7] S. Ganga, M.Y. Ansari, N.V. Ganesh, and A.K.A. Hakeem, "MHD radiative boundary layer flow of nanofluid past a vertical plate with internal heat generation/absorption, viscous and ohmic dissipation effects," Journal of the Nigerian Mathematical Society, **34**, 181-194 (2015). <https://doi.org/10.1016/j.jnms.2015.04.001>
- [8] M.K.A. Mohamed, N.A.Z. Noar, M.Z. Salleh, and A. Ishak, "Mathematical model of boundary layer flow over a moving plate in a nanofluid with viscous dissipation," Journal of Applied Fluid Mechanics, **9**(5), 2369-2377 (2016). <https://doi.org/10.18869/acadpub.jafm.68.236.25247>

- [9] M. Goyal, and R. Bhargava, "Simulation of natural convective boundary layer flow of a nanofluid past a convectively heated inclined plate in the presence of magnetic field," *Int. J. Appl. Comput. Math.*, **4**, 63 (2018). <https://doi.org/10.1007/s40819-018-0483-0>
- [10] P. Rana, B. Mahanthesh, J. Mackolil, and W. Al-Kouz, "Nanofluid flow past a vertical plate with nanoparticle aggregation kinematics, thermal slip and significant buoyancy force effects using modified Buongiorno model," *Waves in Random and Complex Media*, **34**, 3425-3449 (2021). <https://doi.org/10.1080/17455030.2021.1977416>
- [11] S. Dey, S. Mukhopadhyay, and K. Vajravelu, "Nonlinear natural convective nanofluid flow past a vertical plate," *Numerical Heat Transfer, Part A: Applications*, 1-23 (2024). <https://doi.org/10.1080/10407782.2024.2302966>
- [12] K. Padmaja, and R.B. Kumar, "Viscous dissipation and chemical reaction effects on MHD nanofluid flow over a vertical plate in a rotating system. *ZAMM-J Appl Math Mech.* **103**(3), e202200471 (2023). <https://doi.org/10.1002/zamm.202200471>
- [13] K. Padmaja, and R.B. Kumar, "Higher order chemical reaction effects on Cu-H<sub>2</sub>O nanofluid flow over a vertical plate," *Sci. Rep.* **12**, 17000 (2022). <https://doi.org/10.1038/s41598-022-20155-1>
- [14] S. Dey, S. Ghosh, and S. Mukhopadhyay, "MHD mixed convection chemically reactive nanofluid flow over a vertical plate in presence of slips and zero nanoparticle flux," *Waves in Random and Complex Media*, 1-20 (2023). <https://doi.org/10.1080/17455030.2022.2148014>
- [15] A.K. Pati, A. Misra, and S.K. Mishra, "Effect of electrification of nanoparticles on heat and mass transfer in boundary layer flow of a copper water nanofluid over a stretching cylinder with viscous dissipation," *JP journal of heat and mass transfer*, **17**(1), 97-117 (2019). <http://dx.doi.org/10.17654/HM017010097>
- [16] S. Panda, A. Misra, S.K. Mishra, and A.K. Pati, "Flow and Heat Transfer Analysis of H<sub>2</sub>O-Al<sub>2</sub>O<sub>3</sub> Nanofluid Over a Stretching Surface with Electrified Nanoparticles and Viscous Dissipation," *Advances in Dynamical Systems and Applications*, **16**(2), 1533-1545 (2021).
- [17] A.K. Pati, A. Misra, and S.K. Mishra, "Heat and mass transfer analysis on natural convective boundary layer flow of a Cu-Water nanofluid past a vertical flat plate with electrification of nanoparticles," *Advances and Applications in Fluid Mechanics*, **23**(1), 1-15 (2019). <http://dx.doi.org/10.17654/FM023010001>
- [18] A.K. Pati, A. Misra, and S.K. Mishra, "Effect of electrification of nanoparticles on natural convective boundary layer flow and heat transfer of a Cu-Water nanofluid past a vertical flat plate," *International Journal of Engineering, Science and Mathematics*, **6**(8), 1254-1264 (2017). [https://www.ijmra.us/project%20doc/2017/IJESM\\_DECEMBER2017\\_Special\\_Issue/4553\\_pdf.pdf](https://www.ijmra.us/project%20doc/2017/IJESM_DECEMBER2017_Special_Issue/4553_pdf.pdf)
- [19] R. Pattnaik, A. Misra, S.K. Mishra, K.K. Pradhan, S. Panda, and A.K. Pati, "Thermal performance analysis of nanofluid past an exponentially stretching surface due to the electrification effect of nanoparticles," *International Journal of Difference Equations (IJDE)*, **16**, 189-203 (2021). <https://www.ripublication.com/ijde21/v16n2p02.pdf>
- [20] A.K. Pati, S. Mishra, A. Misra, and S.K. Mishra, "Heat and mass transport aspects of nanofluid flow towards a vertical flat surface influenced by electrified nanoparticles and electric Reynolds number," *East Eur. J. Phys.* (2), 234-241 (2024). <https://doi.org/10.26565/2312-4334-2024-2-22>
- [21] A.K. Pati, A. Misra, S.K. Mishra, S. Mishra, R. Sahu, and S. Panda, "Computational modelling of heat and mass transfer optimization in copper water nanofluid flow with nanoparticle ionization," *JP Journal of Heat and Mass Transfer*, **31**, 1-18 (2023). <https://doi.org/10.17654/0973576323001>
- [22] H.F. Oztop, and E. Abunada, "Numerical study of natural convection in partially heated rectangular enclosures filled with nanofluids," *International Journal of Heat Fluid Flow*, **29**, 1326-1336 (2008). <https://doi.org/10.1016/j.ijheatfluidflow.2008.04.009>
- [23] U. Farooq, H. Waqas, A. Bariq, S.K. Elagan, N. Fatima, M. Imran, S.A. Khan, et al., "Local similar solution of magnetized hybrid nanofluid flow due to exponentially stretching/shrinking sheet," *BioNanoSci.* **14**, 368-379 (2024). <https://doi.org/10.1007/s12668-023-01276-x>
- [24] A. Bejan, *Convection Heat Transfer*, (Wiley, New York, 1984).

#### ХІМІЧНА РЕАКЦІЯ, ЕЛЕКТРИЗАЦІЯ, БРОУНІВСЬКИЙ РУХ ТА ТЕРМОФОРЕЗНИЙ ЕФЕКТ НАНОЧАСТИНОК МІДІ НА ПОТОК НАНОРІДИНИ З ПОВЕРХНЕВИМ ТЕРТЯМ, ТЕПЛО-ТА МАСОПЕРЕНОСОМ

Адїтья Кумар Патї<sup>а</sup>, Мадан Мохан Роут<sup>а</sup>, Руну Саху<sup>б</sup>, І. Сїва Рамакотї<sup>а</sup>, Коустав Кумар Панда<sup>а</sup>, Крушна Чандра Сетї<sup>а</sup>

<sup>а</sup>Університет технології та менеджменту Центуріон, Паралахемунді, Одїша, Індїя

<sup>б</sup>Університет NIST, Берхамтур, Ганджам, Одїша, Індїя

У цьому дослідженні досліджується вплив хімічної реакції першого порядку, термофорезу, електризації та броунівського руху на наночастинки Cu у вільному конвективному потоці нанофлюїду повз вертикальну плоску поверхню, з тертям поверхні, тепло- та масообміном. Унікальне поєднання хімічної реакції та ефектів електризації відрізняє це дослідження від попередніх досліджень потоку нанорідини. Використовуючи функції подібності, керуючі PDE потоку перетворюються на систему локально подібних рівнянь. Потім ці рівняння розв'язуються за допомогою функції `bvp4c` MATLAB, що включає безрозмірні граничні умови. Висновки підтверджуються шляхом порівняння з попередніми дослідженнями. Графічні ілюстрації показують чисельні дослідження профілів концентрації, швидкості та температури у зв'язку з параметром електризації, параметром термофорезу, параметром хімічної реакції та параметром броунівського руху. Результати розрахунків коефіцієнтів теплообміну, масообміну та безрозмірного шкірного тертя подано у вигляді таблиці. Основне відкриття вказує на те, що параметр електризації прискорює передачу тепла, тоді як параметр електризації, параметр броунівського руху та параметр хімічної реакції збільшують швидкість передачі маси від плоскої поверхні до нанорідини. Це вказує на обнадійливий потенціал для охолодження плоских поверхонь у промисловості.

**Ключові слова:** хімічна реакція; термофорез; електрифікація; броунівський рух; нанофлюїд